

Fusion Bonding of Supercooled Poly(ethylene terephthalate) Between T_g and T_m

Ruihua Li,¹ Donggang Yao,¹ Qunhui Sun,^{2*} Yulin Deng²

¹School of Polymer, Textile and Fiber Engineering, Georgia Institute of Technology, Atlanta, Georgia 30332

²School of Chemical and Biomolecular Engineering, Georgia Institute of Technology, Atlanta, Georgia 30332

Received 29 December 2009; accepted 13 July 2010

DOI 10.1002/app.33070

Published online 22 September 2010 in Wiley Online Library (wileyonlinelibrary.com).

ABSTRACT: Because of its slowly crystallizing nature, poly(ethylene terephthalate) (PET) can be supercooled into an amorphous glass by rapid quenching. Upon reheating between T_g and T_m , the amorphous PET are subjected to two competing processes: rubber softening and crystallization. Fusion bonding of two such crystallizable amorphous polymer sheets in this processing temperature window is thus a complex process, different from fusion of purely amorphous polymer above T_g or semicrystalline polymer above T_m . In this study, the interfacial morphological development during fusion bonding of supercooled PET in the temperature window between T_g and T_m was studied. A unique double-zone interfacial morphology was observed at the bond. Transcrystals were found to nucleate at the interface and grow inward toward the bulk and appeared

to induce nucleation in the bulk to form a second interfacial region. The size and morphology of the two zones were found to be significantly affected by the fusion bonding conditions, particularly the fusion temperature. The fusion bonding strength determined by the peeling test was found to be significantly affected by the state of crystallization and the morphological development at the bonding interface. Based on the interfacial morphology observed and the bonding strength measured, a fusion bonding mechanism of crystallizable amorphous polymer was proposed. © 2010 Wiley Periodicals, Inc. *J Appl Polym Sci* 119: 3101–3112, 2011

Key words: single-polymer composites; homocomposites; slowly crystallizing polymers; polyethylene terephthalate; fusion bonding

INTRODUCTION

Single-polymer composites¹ are composites with matrix and reinforcement (typically fibers) made from the same polymer. It is well known that the strength and modulus of polymer are highly structure-dependent. Bulk pieces of polymer, due to the lack in orientation and/or crystallization, typically have a modulus ~ 1 GPa and a strength of 50 MPa or below, while highly oriented and highly crystalline polymer fibers can have a tensile modulus well above 10 GPa and a tensile strength well above 1 GPa. This large contrast offers opportunities to design and manufacture single-polymer composites (SPCs) with enhanced mechanical properties. More importantly, because a single polymer is employed, SPCs hold the promise for improved fiber-matrix compatibility and enhanced recyclability.² Despite these advantages, SPCs are difficult to be processed

using standard polymer processing techniques. Should a melt process (e.g., extrusion or molding) be used for processing a single-polymer composite, the fiber properties would be deteriorated or even the fibers would be melted. Therefore, special techniques for consolidating the single-polymer hybrid and yet preserving the useful properties of the reinforcement are needed in SPCs processing. So far, the work in SPCs processing has been primarily focused on a fiber hot compaction process,^{3–5} where polymer fibers or fabrics are compacted at a temperature very close to, but below, the polymer melting temperature so as to partially melt the fiber and fuse them into a single solid material. The major challenge in this process is the small difference, typically less than 10°C, between the feasible processing temperature and the fiber melting temperature. Within such a small temperature window, it is difficult to process the SPC under normal processing conditions without significantly annealing the fiber. It is known that polymer fibers annealed at a temperature close to their melting temperature results in a much reduced modulus toward that of the unoriented polymer.⁶

Recently, Yao et al.^{7,8} proposed to use slowly crystallizing polymers for enlarging the processing temperature window. In this process, supercooled polymer is re-heated between T_g and T_m to soften and

*Present address: New Span Opto-Technology Inc., 16115 SW 117 Ave., A-15, Miami, FL 33177.

Correspondence to: D. Yao (yao@gatech.edu).

Contract grant sponsor: CCACTI (Consortium on Competitiveness for the Apparel, Carpet, and Textile Industry) Program in Georgia.

fuse into a matrix material for encapsulating highly oriented, highly crystalline fibers of the same polymer. This method was successfully applied to two slowly crystallizing polymers, namely, poly(ethylene terephthalate) (PET) and poly(L-lactic acid). Particularly in the PET case, a processing temperature window as large as 70°C was obtained. The experimental results, however, also indicated that the matrix fusion quality is highly sensitive to the process parameters, especially the temperature history during fusion.

It is well-known that, upon rapid quenching to a temperature below the glass transition temperature (T_g), slowly crystallizing polymers such as PET can be supercooled into a nearly amorphous glass. When re-heated between T_g and the melting temperature (T_m), the supercooled glass is subjected to two competing processes. First, the amorphous phase will experience a glass transition at T_g , and the polymer becomes rubbery and sticky in the rubbery plateau region between T_g and T_m . Two such sticky pieces can be fused together through chain diffusion at the interface. The second competing process is crystallization. For a crystallizable amorphous phase, such as an amorphous PET phase, it crystallizes over a wide temperature range between T_g and T_m . Therefore, the just softened, rubbery, and sticky amorphous phase turns into a hardened crystalline phase at the same processing temperature. Because of these competing processes, the fusion process of supercooled polymer between T_g and T_m is more complex than standard fusion bonding involving either amorphous polymer above T_g or semicrystalline polymer above T_m . The crystallization kinetics and the resulting interfacial morphology are expected to strongly affect the fusion bonding quality. This fusion process is not only fundamentally interesting but also technically important. Besides applications in SPCs processing, understanding of this fusion process may lead to new technical developments in polymer welding and sealing. Unfortunately, there are few studies, if any, on this topic, and related knowledge is little.

In this study, supercooled amorphous PET sheets were reheated and fusion-bonded at a processing temperature between T_g and T_m . Note that this experimental protocol is different from that used in standard fusion where PET is heated above T_m . In the conventional process, the interface is healed mainly above T_m where crystallization is absent. However, in the present experiment, healing and crystallization are two parallel processes, and their interaction can affect both interfacial morphology and fusion quality. On one hand, an unhealed interface can alter the nucleation rate and crystallization kinetics.⁹⁻¹¹ On the other hand, concurrent crystallization can retard molecular diffusion and reduce the

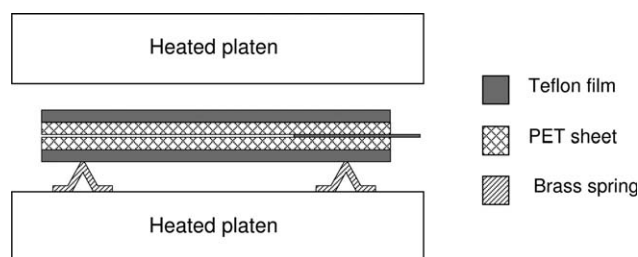


Figure 1 Experimental setup for fusion bonding of two polymer sheets.

healing rate at the interface. The main objective of this study is, therefore, to characterize the morphology at the interface and its vicinity and the resulting fusion bonding strength, leading to increased understanding on the interplay between interfacial morphology and fusion bonding quality.

EXPERIMENTAL

Sample preparation

PET sheets, 0.25 mm in thickness, produced by melt extrusion and rapid cooling against a room-temperature metal roll, were used in the experiment. The number and weight averaged molecular weights of the PET polymer are $\sim 27,000$ and $41,000 \text{ g mol}^{-1}$. T_g and T_m of this polymer are ~ 70 and 260°C , determined by differential scanning calorimetry (DSC). The crystallinity of the PET sheet as measured by DSC is less than 0.5%, indicating a nearly amorphous polymer. Two amorphous PET sheets, $50 \times 50 \text{ mm}^2$ in area, were fusion-bonded under heat and pressure using a heated hydraulic press. The experimental setup is schematically shown in Figure 1. Thin Teflon[®] films (0.07 mm in thickness) were used on both sides for easy mold separation. An additional Teflon film was employed in the middle of the lamination to create an unbonded region for peeling testing. Precision shims of a thickness of 0.56 mm were inserted between the heated platens to control the thickness of the bonded sheet. This yielded a final thickness of 0.42 mm for the bonded PET sheet. The compression pressure was set approximately to 1 MPa. The platen temperature was varied between T_g and T_m , and the holding time was varied from 0 to 90 s. The isothermally-fused PET sheet obtained from this procedure was rapidly quenched into tap water to obtain a fully solidified sample for morphological characterization and peeling test.

It should be noted that the laminations used in the above experiments are very thin, on the order of 0.5 mm. Therefore, the samples were rapidly heated to the target temperature within a very short period. For supercooled PET films, the typical density, thermal conductivity, and specific heat are 1.35 g cm^{-3} ,

$0.3 \text{ W m}^{-1} \text{ }^\circ\text{C}^{-1}$, and $1300 \text{ J kg}^{-1} \text{ }^\circ\text{C}^{-1}$. By defining a dimensionless temperature $T^* = (T - T_h)/(T_0 - T_h)$, where T_h is the heating temperature and T_0 is the initial temperature of the PET film, and assuming negligible contact resistance, one would estimate a heating time of less than 0.05 s for the center of the lamination to reach $T^* = 0.9$. This level of heating time is considerably smaller than the crystallization time scale of PET and therefore its effect on morphological development was not considered in this study.

Characterization

After fusion bonding, the bonded sheets were cut into $1 \text{ cm} \times 4 \text{ cm}$ rectangles. These rectangles were then sliced into stripes with $500 \text{ }\mu\text{m}$ thickness. The surfaces of the resulting samples were etched with a 2 wt % potassium hydroxide/isopropanol solution for 4 h at room temperature. Then these samples were washed by isopropanol, extracted in ethylene glycol for 24 h, and afterward washed by acetone and water in sequence. Amorphous PET is expected to be more easily etched by the solvent than crystalline PET, and therefore a topographical contrast can be created on the etched surface. The etched and washed specimens were dried at room temperature and then coated with a fine gold layer by ion-sputtering for examination on a S-800 SEM system (low resolution) and a LEO 1530 SEM system (high resolution). The bonded sheets were also sliced by microtome for transmission electron microscopy (TEM) and polarized optical microscopy. TEM was performed on a Hitachi HF2000 TEM system. For optical microscopy, an Olympus BH-2 optical microscope was used. All optical micrographs presented in this chapter were taken under crossed polarizers.

The bonding developed after compaction and fusion was evaluated using a T-peel test (according to ASTM D1876). The width of the peeling samples is 10 mm. The peel tests were carried out at a displacement rate of 20 mm min^{-1} on an Instron tensile testing machine.

RESULTS AND DISCUSSION

Interfacial morphology

The interfacial morphologies of the fused sheets under different holding times at 180°C are showed in Figure 2. Two distinct zones were observed in the vicinity of the interface: an inner zone of a characteristic size of $2 \text{ }\mu\text{m}$ and an outer zone of a characteristic size of $30 \text{ }\mu\text{m}$. The actual size and appearance of the outer zone were affected by the holding time. At a short holding time, e.g., 10 s, the boundary between the outer zone and the bulk polymer can be

clearly seen. This boundary became less distinguishable at longer holding time, e.g., 60 s. The overall size of the outer zone appeared to be larger at the shorter holding time.

The inner zone right at the interface was imaged using higher magnification and the morphology is separately shown in Figure 3. After etching, the remaining crystalline material at the interface formed many tiny bridges connecting the two sides of the interface. Note that this transcrySTALLINE region was formed at an exceptionally short holding time, e.g., less than 10 s, considerably smaller than the characteristic half-time of crystallization for PET, about 40 s at 180°C .^{7,12} With the increase of the holding time, the transcrySTALLINE region appeared to grow denser [comparing Fig. 3(a) with Fig. 3(b)]. The growth of this transcrySTALLINE region over time is understandable from basic crystal growth kinetics. However, the rapid formation of the transcrySTALLINE region at a very short heating time, e.g., less than 10 s, indicated the presence of nucleation effects at the interface.

Heterogeneous nucleation is often triggered by interfaces provided, e.g., by surface, foreign species, and impurities such as catalysts, dust particles, and additives.⁹ Particularly, the surface of a specimen can serve as a heterogeneous nucleus.¹³ Thus, the contact interface between two polymer films can trigger crystal nucleation. Because of the geometric nature of the polymer molecule, the surface-nucleated crystal tends to grow with the chain axis parallel to the surface for maximum reduction of free energy. The fastest crystal growth direction should be normal to the surface.¹³ Figure 4 is a schematic illustration of the transcrySTALLINE microstructure model. The lamellae grow outward in the direction perpendicular to the contact interface. This heterogeneous nucleation and transcrySTALLINE growth theory can be used to explain the unique morphology at the PET-PET interface observed in this study. It can be seen from Figure 3 the growth direction of crystals at the interface was perpendicular to the interface. The transcrySTALLINE region was formed at a very short time scale, $\sim 5 \text{ s}$. This time scale is much shorter than the quiescent crystallization time scale of PET. However, at the initial stage, the transcrySTALLINITY appeared to be low, with relatively thin transcrySTALLINE crystals at the contact interface [cf., Fig. 3(a)]. With the increase of the heating time, the transcrySTALLINE region became denser and the visible void space (corresponding to the etched amorphous polymer) at the interface was smaller.

Figure 2 also reveals that, besides the transcrySTALLINE zone, there existed a second interfacial region. Different reasons may be used to explain the formation of this second zone. However, it is highly likely that the transcrySTALLINE crystals at the interface may cause

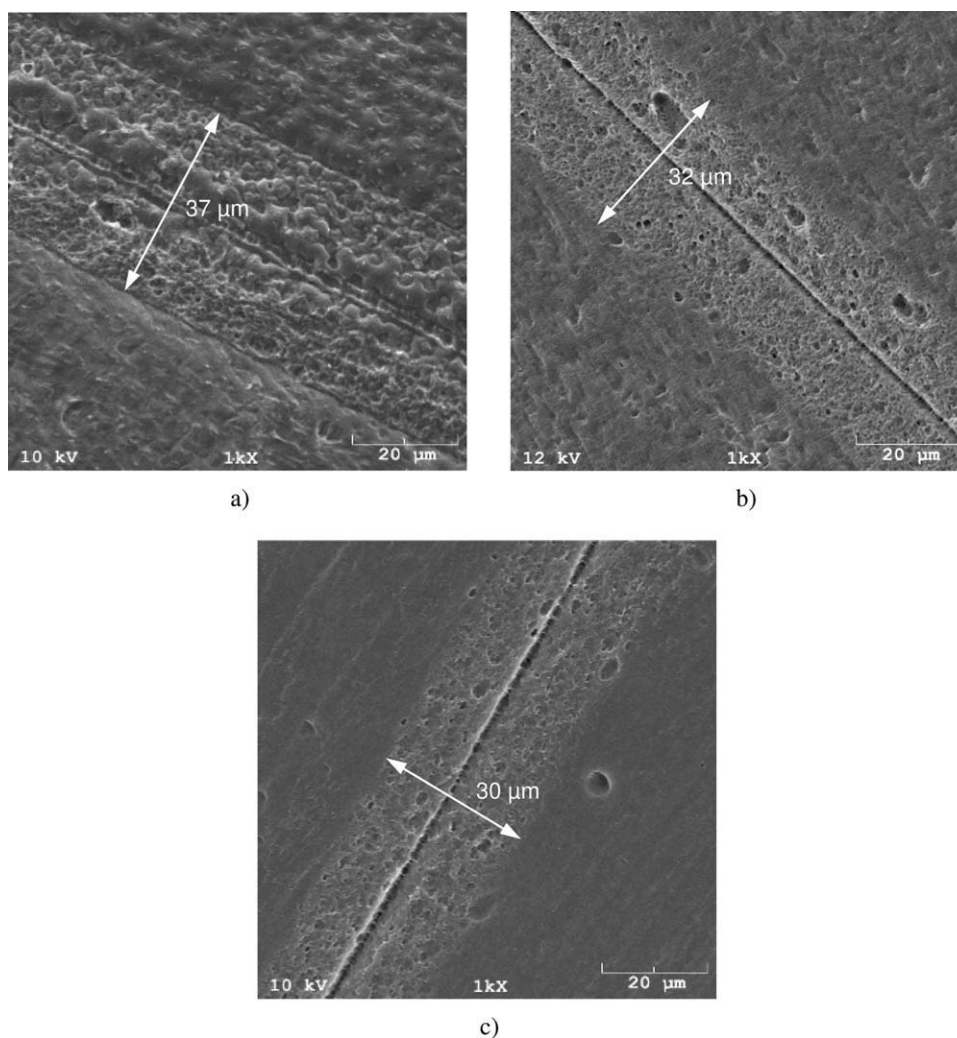
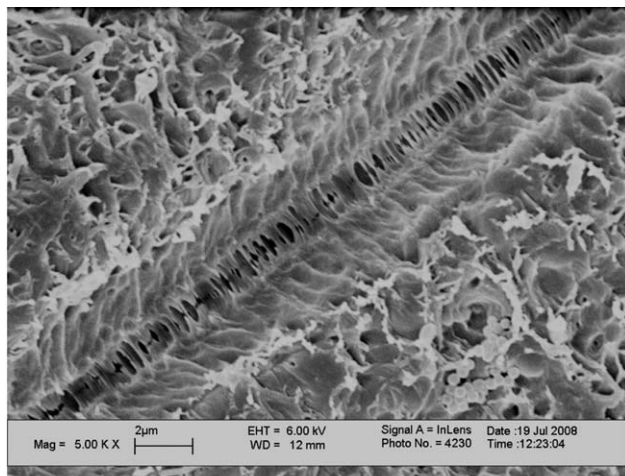


Figure 2 Interfacial bonding morphology of two crystallizable amorphous PET sheets. The PET sheets were fused at heating temperature 180°C with different holding times: (a) 10 s, (b) 30 s, and (c) 60 s. The sample was etched by 2 wt % potassium hydroxide/isopropanol solution for 4 h.

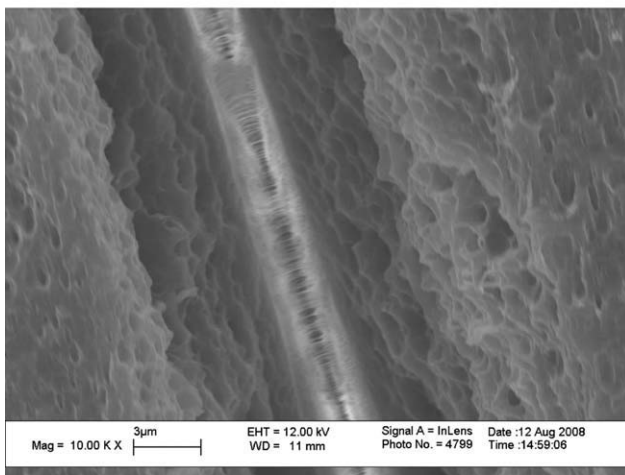
nucleation in the surrounding material. Note that the nucleation of this type would be anisotropic and directional, different from the homogeneous nucleation in the bulk far away from the interface. Thus, the crystalline region in the neighborhood of the interface may bear a distinct morphology compared with that in the bulk, resulting in the formation of the second interfacial zone. The crystals in the inner interfacial region may keep growing until the growing front is impeded by the crystal growth in the second interfacial zone. For the PET-PET interface, in fact, a distinct boundary was observed between the two zones after a long period of growth, as shown in Figure 3(b). Likewise, the growth of the crystals in the second interfacial zone may be hindered by the homogeneous crystal growth in the bulk. This causes the formation of the other boundary of the second interfacial zone. In addition to anisotropic nucleation effects, heat transfer may provide a driving force for formation of the second interfa-

cial region. When the samples were heated, the heat was transferred from outside to the interface. There could be a temperature gradient in the thickness direction, particularly when relatively large interfacial thermal resistance should be involved. However, such nonisothermal effects are expected to be low due to the small thickness of the films used in the experiments.

Figure 2 also shows that with the increase of the heating time, the total width of the double interfacial zone decreased. The reduction in width was rapid at the beginning but slowed down in the later stage. The crystallinity and the properties of the second interfacial zone are expected to be more similar with the bulk than with the transcristalline region at the interface. This is supported by the relatively lower contrast in morphology between the second zone and the bulk, as observed on the etched sample. With the increase of the heating time, the molecular chains and crystals may rearrange themselves in the



a)



b)

Figure 3 Transcrystalline morphology of two crystallizable amorphous PET sheets. The PET sheets were fused at heating temperature 180°C with different heating times: (a) 10 s and (b) 60 s. The sample was etched by 2 wt % potassium hydroxide/isopropanol solution for 4 h.

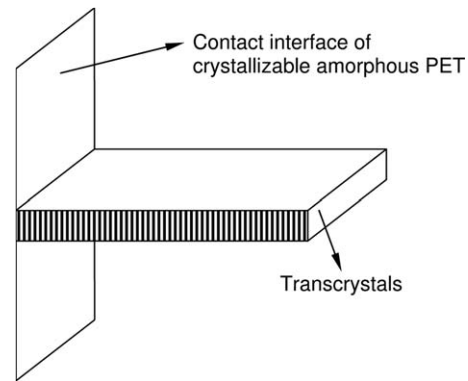
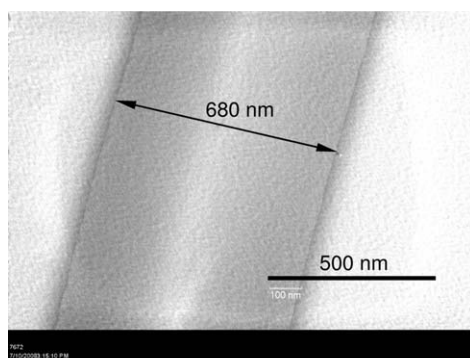


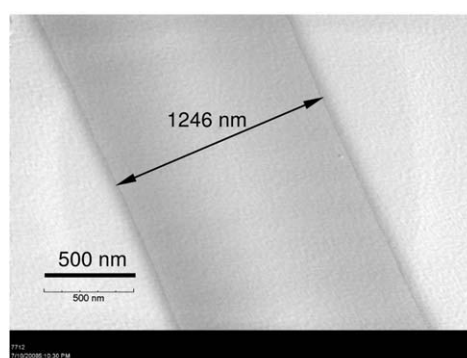
Figure 4 Schematic illustration of transcrystals microstructure model.

second zone. Thus, healing effects may be presented at the boundary between the second zone and the bulk, resulting in reduction of the width of the second interfacial zone.

The interfacial bonding region of two crystallizable amorphous PET sheets was also observed using TEM. Representative TEM micrographs for samples bonded at 180°C with varied holding time are shown in Figure 5. From the TEM micrographs, it is seen that the shades of the interfacial region and the surrounding region were different; the interfacial region was darker. The width of the interfacial region, on the order of 1 µm, was comparable to that of the first interfacial zone observed by SEM. Thus the darker interfacial region in the TEM pictures was deemed as the transcrystalline region in the interfacial zone. Typically in TEM, higher crystallinity and density gives rise to a darker appearance. The darker appearance of the transcrystalline region, therefore, indicated relatively higher crystallinity in this region. The darker region was found to form at a short holding time of 5 s [Fig. 5(a)]. As the holding time increased from 5 to 20 s, the overall size of the darker region grew by nearly two times, indicating



a)



b)

Figure 5 TEM images of the interfacial zone of two crystallizable amorphous PET sheets fused at heating temperature 180°C with different heating times: (a) 5 s and (b) 20 s.

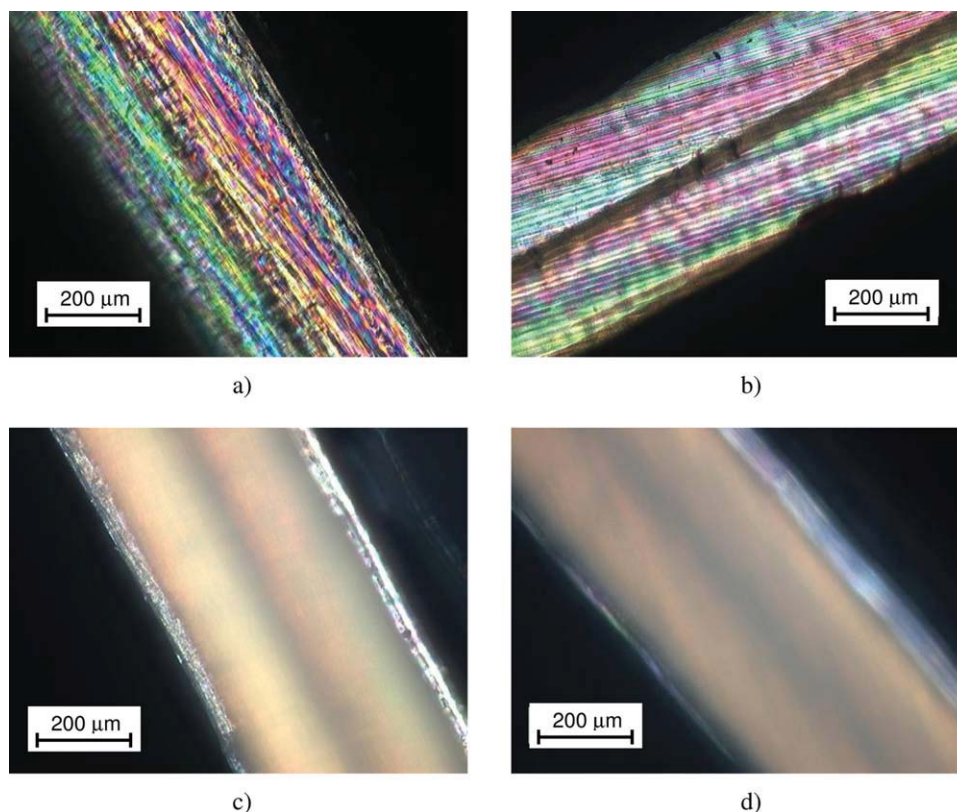


Figure 6 Polarized micrographs of the interfacial zone of two crystallizable amorphous PET sheets bonded at heating temperature 180°C with different heating times: (a) 5 s, (b) 10 s, (c) 20 s, and (d) 30 s. [Color figure can be viewed in the online issue, which is available at wileyonlinelibrary.com.]

the growth of the transcrystals in the perpendicular direction to the interface. It was also observed that, the center of the interfacial zone appeared to be slightly brighter than the neighboring material. Because of geometrical symmetry, this brighter center should correspond to the original contact interface between the two PET sheets. The resulting low crystallinity in the center agreed with the relatively amorphous center (with spaces left after etching) at the contact interface observed in the SEM micrographs (Fig. 3). The varied crystallization rate in the interfacial region may be caused by preferential crystal growth and relatively low degree of chain diffusion at the interface. This phenomenon is worth a focused future study to obtain a more quantitative understanding.

Polarized optical microscopy in Figure 6 also indicates the existence of the distinct interfacial zone at the PET–PET bonding interface, particularly for samples bonded with short heating times. The width of the interfacial zone observed by polarized optical microscopy is comparable to that of the second interfacial region in the SEM. The colorful zones on samples with short heating times, e.g., 10 s, were caused by the uneven scratches of knife on the cutting surface. These scratches gave rise to birefringence, and therefore colorful fringes, when the sample was

observed with polarized light. The scratch marks were confirmed by transmission microscopy without polarized light; without polarization, the scratch marks were clearly observed. The center zones in Figure 6(a) or (b), corresponding to the interfacial zones, had a more uniform surface appearance on the cutting surface; therefore, with polarized light, it showed a small amount of birefringence and appeared dark. The different appearance on the same cutting surface may be attributed to the variation of the mechanical properties on the cross section of the PET sample. When the heating time was shorter, the crystallinity of the bulk was low. Thus the modulus of the bulk would be lower than that of the interfacial zone. In fact, for fast crystallizing polymers, several previous papers^{14–17} have already reported that the modulus of the transcrystalline region is higher than that of the bulk phase. The bulk material would thus be easier to be scratched during slicing, while the hard interfacial transcrystalline region would be more resistant to scratches. Figure 6 also illustrates the effect of heating time on the cutting surface appearance. As the heating time increased, the difference in appearance diminished. For example, the sample prepared with a long heating time of 30 s showed a uniform appearance under the polarized optical microscope [Fig. 6(d)]. This

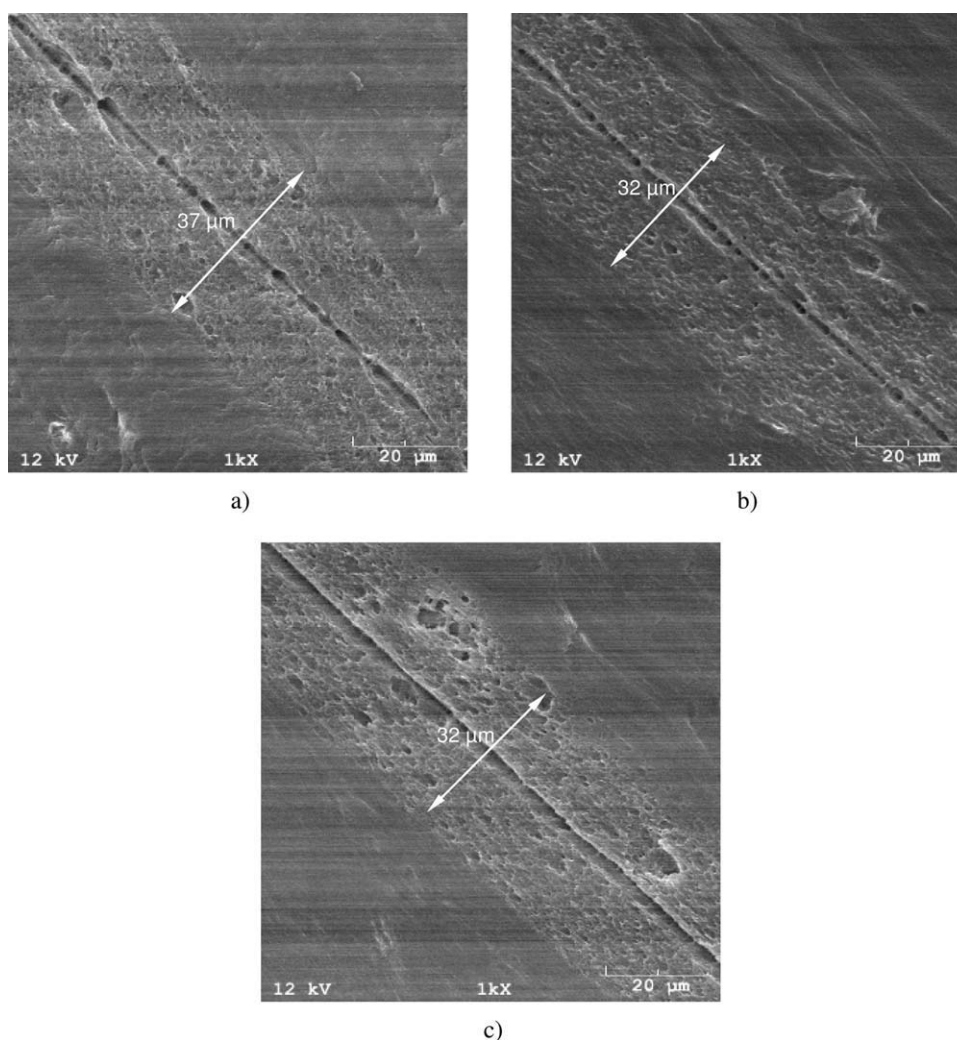


Figure 7 Interfacial bonding morphology of two crystallizable amorphous PET sheets etched by 2 wt % potassium hydroxide/isopropanol solution for 4 h. The PET sheet was fused at heating temperature 160°C with different heating times: (a) 10 s, (b) 30 s, and (c) heating time 60 s.

change in cross-sectional appearance with heating time can again be attributed to crystallization; with increased crystallinity at longer heating times, the crystallinity of the bulk material increased, thus providing improved resistance to scratches.

The double interfacial regions were also observed on samples prepared at both lower and higher heating temperatures, as shown in Figures 7 and 8. The interfacial morphology changed in different ways at different temperatures. At the lower heating temperature of 160°C, the width of the interfacial region stabilized at an intermediate heating time of 30 s and did not change significantly afterward. At the higher heating temperature of 210°C, the width of the interfacial region decreased more rapidly with the increase of the heating time. An explanation for the different responses to the change in heating time is given below. Upon heating above T_g , the amorphous PET becomes a rubbery material. However, at this same temperature, the amorphous PET also

crystallizes. When the heating temperature was low, e.g., 160°C, the mobility of the molecular chain in amorphous region was relatively low; yet, crystallization was still as comparably fast as with a higher heating temperature, as inferred from the bell shape of crystallization half-time for PET.¹² As a result, the change in morphology due to rearrangement of intercrystal chains would be slow at this low heating temperature. At a higher heating temperature, e.g., 210°C, the mobility of the molecular chains would be much higher. Therefore, more annealing effects would be expected at higher temperature, resulting in homogenization of morphology between dissimilar crystalline regions. It is thus understandable that, the higher the heating temperature, the faster the width of the interfacial region decreased.

The interfacial morphology of samples prepared at 160° and 210°C was also studied using TEM and polarized microscopy. The results are shown in Figures 9–12. These results were similar to those

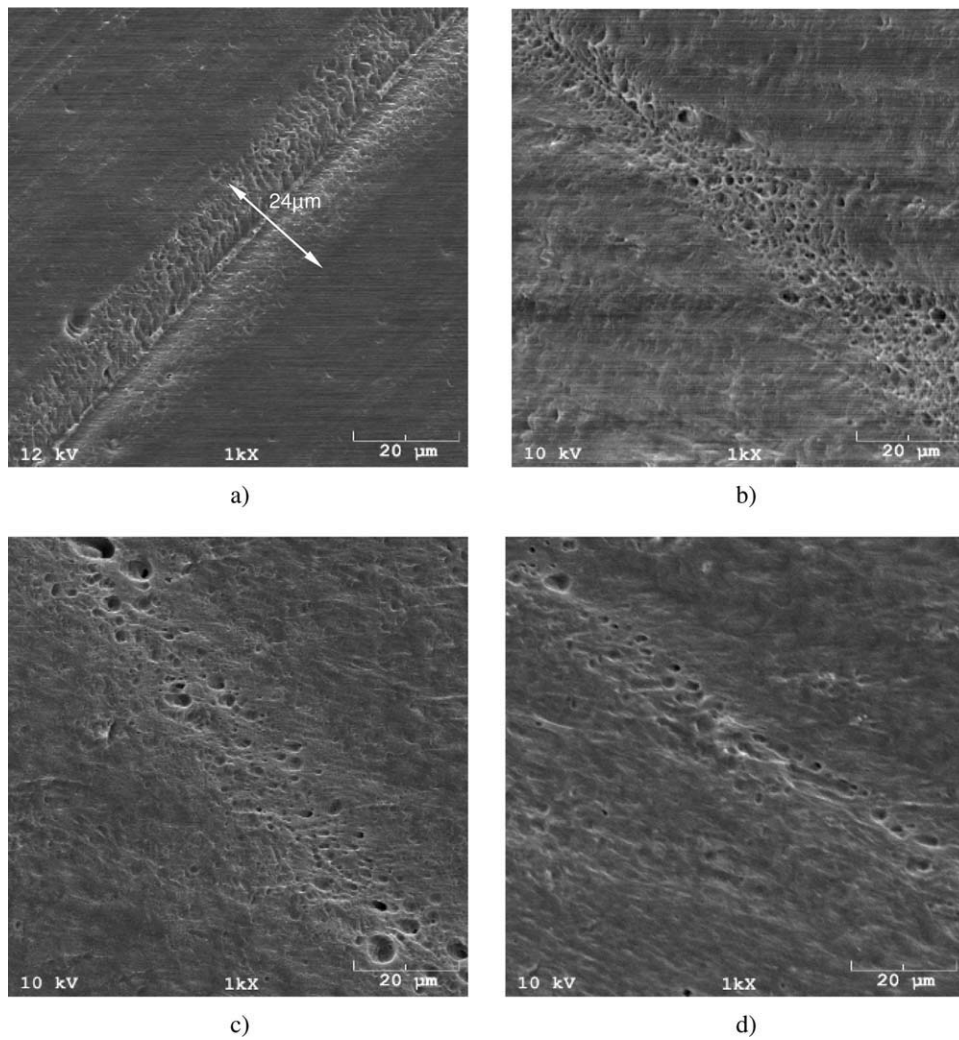


Figure 8 Interfacial bonding morphology of two crystallizable amorphous PET sheets etched by 2 wt % potassium hydroxide/isopropanol solution for 4 h. The PET sheet was fused at heating temperature 210°C with different heating times: (a) 10 s, (b) 30 s, (c) 60 s, and (d) 90 s.

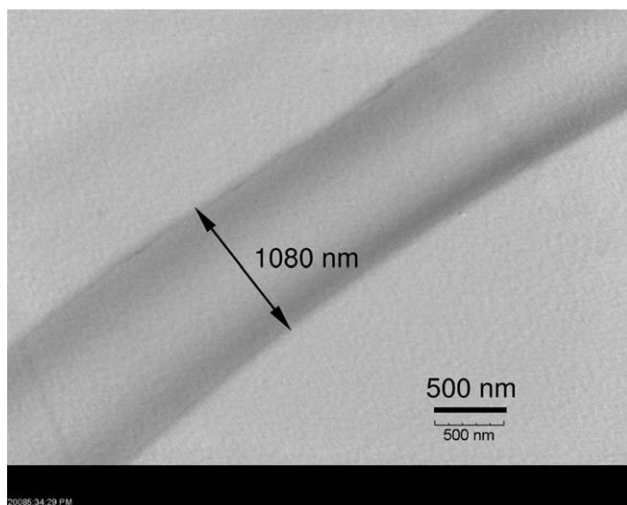


Figure 9 TEM image of the interfacial zone of two crystallizable amorphous PET sheets fused at heating temperature 210°C and heating time 60 s.

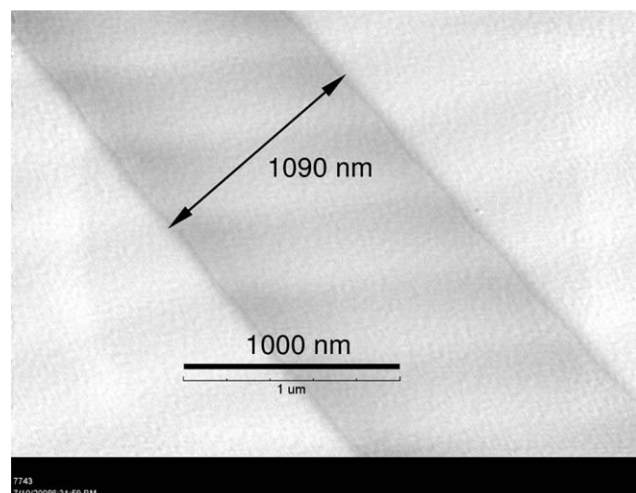


Figure 10 TEM image of the interfacial zone of two crystallizable amorphous PET sheets fused at heating temperature 160°C with heating time 60 s.

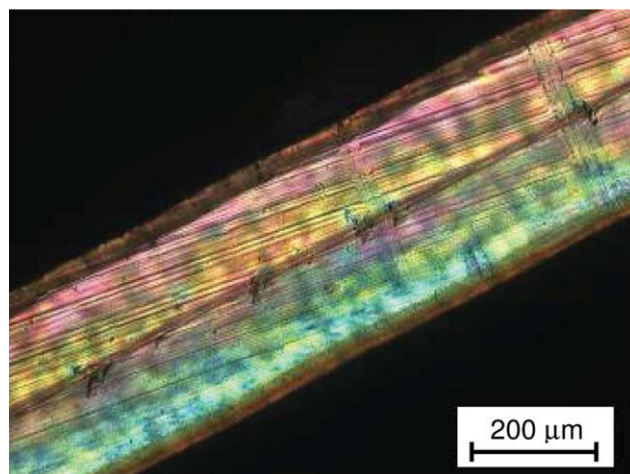


Figure 11 Optical micrograph of the interfacial zone of two crystallizable amorphous PET sheets fused at heating temperature 210°C with heating time 30 s. [Color figure can be viewed in the online issue, which is available at wileyonlinelibrary.com.]

observed on the sample fused at 180°C. Again, the interfacial zone in TEM corresponded to the trans-crystalline region in SEM, while in polarized microscopy it was correlated with the second interfacial zone in SEM.

Peeling test results

The fusion bonding behavior of crystallizable amorphous PET under different platen temperature was studied. Three different temperatures were used: 160, 180, and 210°C. Of these temperatures, 160°C was far below the melting temperature of PET, while 210°C was far above the glass transition temperature; 180°C was the intermediate temperature. The effects of the heating time on the peeling strength and the crystallinity (measured by differential scanning calorimetry at a heating rate of 10°C

min⁻¹) at different heating temperature are shown in Figures 13–15.

The results for heating temperature of 160°C are shown in Figure 13. With the increase in heating time, the crystallinity of the PET sheet was increased; however, at the same time, the interfacial bonding strength was decreased. The exact reason for this phenomenon is not clear at this point, but it is possible that long heating times at 160°C resulted in largely coarsened crystals at the interface and therefore a brittle interface. Additionally, crystallinity may affect the fusion bonding between the two PET sheets. At shorter heating time, the polymer sheet is nearly amorphous, and the polymer chain can interdiffuse with each other at the interface. With the increase of the heating time, crystallinity is increased, which in turn reduces the chain mobility at the interface and therefore the interdiffusion rate. Polymer crystallization is the (natural or artificial) process of formation of solid crystals precipitating from an identical solution or melt. After crystallization, the rubbery state of the polymer becomes solid crystals. After the polymer chain is completely frozen by the crystallization, the interdiffusion of the polymer chain at the interface may be stopped. At 160°C, it is likely that the overall effects of crystal coarsening and interdiffusion reduction caused the reduced peeling strength.

The results for heating temperature of 180°C are shown in Figure 14. By average, the peeling strength at 180°C was higher than at 160°C. The influence of the heating time was also found to be different at this increased temperature. At 180°C, with the increase of the heating time, the fusion bonding strength of the crystallizable amorphous PET was increased first and then decreased. An explanation for this behavior is attempted below. At 180°C, the fusion bonding speed is expected to be faster than at 160°C, but the crystallization speed may remain

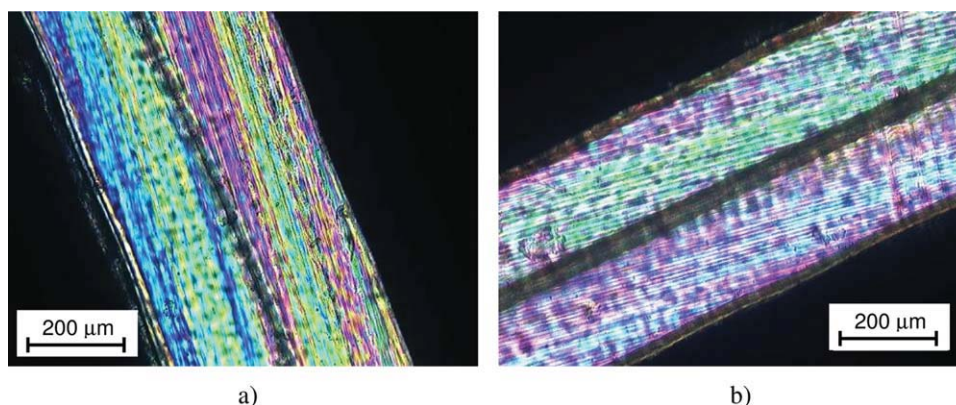


Figure 12 Optical micrographs of the interfacial zone of two crystallizable amorphous PET sheets fused at heating temperature 160°C with different heating times: (a) 5 s and (b) 15 s. [Color figure can be viewed in the online issue, which is available at wileyonlinelibrary.com.]

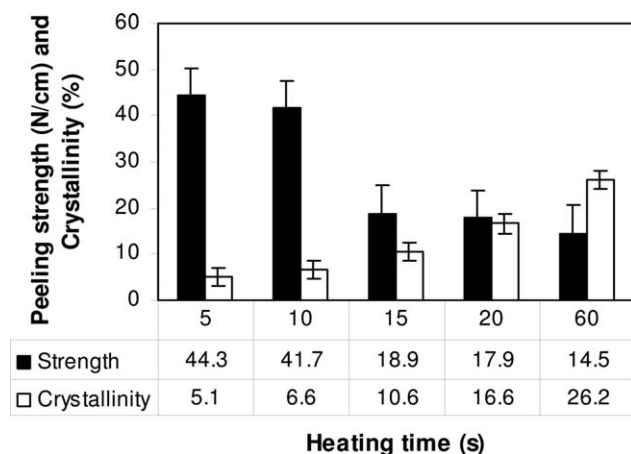


Figure 13 Effect of heating time on the bonding strength at 160°C.

unchanged (known from the typical bell shape for the half-time of crystallization). At the beginning, diffusion was predominant. With the increase of the heating time, the amount of diffusion increased, and the interface and bulk became more uniform, resulting in the increase of the bonding strength. Thus, with the increase of the heating time, the fusion bonding strength was increased at the beginning. When interdiffusion and the crystallization were in balance, the interfacial bonding strength reached the highest. Later, crystallization became predominant. With the increase of the heating time, crystallization may cause a brittle interface, resulting in decreased bonding strength.

The results for heating temperature of 210°C are shown in Figure 15. This heating temperature is much closer to the PET melting temperature than the other two temperatures. At 210°C, the fusion bonding speed is expected to be faster. However, the crystallization speed was slower (known from the bell shape for the half-time of crystallization).

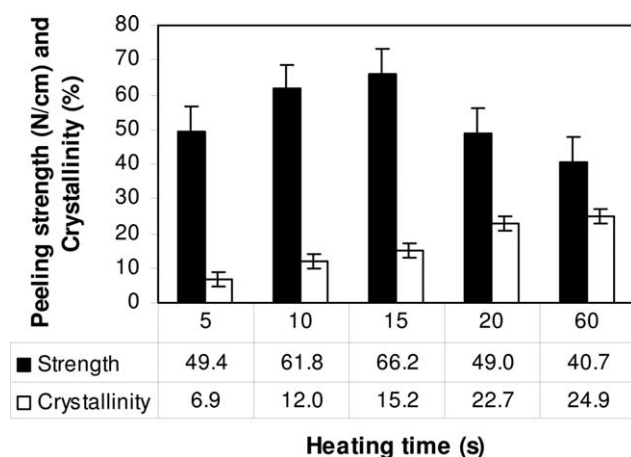


Figure 14 Effect of heating time on the bonding strength at 180°C.

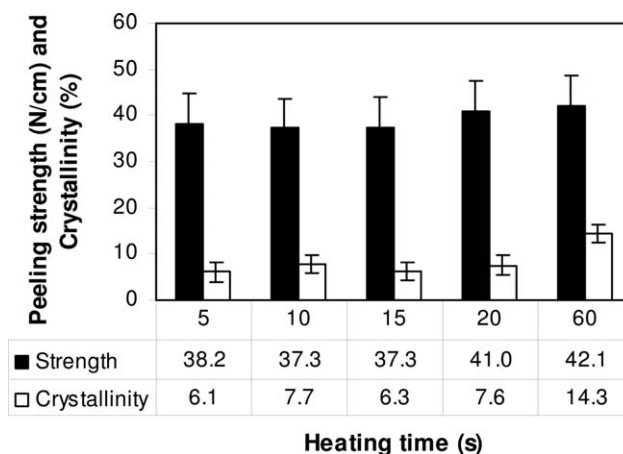


Figure 15 Effect of heating time on the bonding strength at 210°C.

Thus molecular interdiffusion became a more dominant process. With the increase of the heating time, the peeling strength was increased then became stabilized. At this elevated temperature, the fusion bonding behavior of two crystallizable amorphous PET sheets was somewhat similar to that of purely amorphous polymer with heating temperature above T_g . For purely amorphous polymers, previous investigations^{18–21} have shown that the bonding strength increases with the increase of temperature. The bonding strength can also slightly increase with the increase of heating time.

Model of fusion bonding between T_g and T_m

Additional discussion is provided hereinafter with an attempt to formulate a fusion bonding mechanism for the crystallizable amorphous PET. When heat and pressure are applied to two thermoplastic surfaces in contact, the materials are softened by the applied heat. The pressure causes the softened surface to spread, resulting in an intimate contact interface between the thermoplastic surfaces. Then the high temperatures at the interface can make polymer chains across the interface interdiffuse until the materials are cooled down or solidified. Previous studies^{22–24} in fusion bonding of thermoplastics have focused on amorphous polymer with bonding temperatures above T_g and semicrystalline polymer with

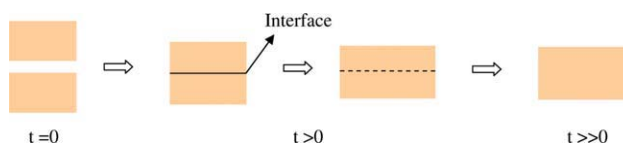


Figure 16 Schematic representation of bonding of two amorphous polymer sheets above T_g ²⁵ or bonding of two crystallized polymer sheets above T_m . [Color figure can be viewed in the online issue, which is available at wileyonlinelibrary.com.]

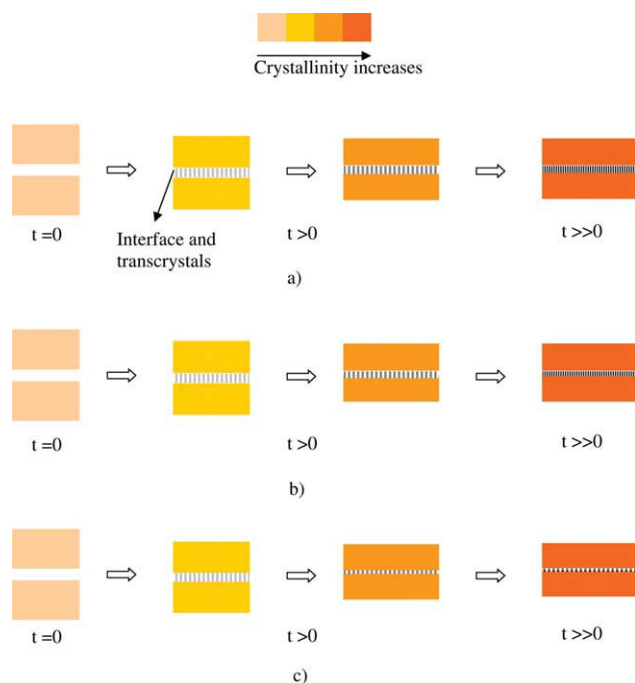


Figure 17 Schematic representation of bonding of two crystallizable amorphous polymer sheets between T_g and T_m when fusion bonding rate is faster than crystallizing rate: (a) low temperature, (b) intermediate temperature, and (c) high temperature (near the melting temperature). [Color figure can be viewed in the online issue, which is available at wileyonlinelibrary.com.]

fusion bonding temperature above T_m . Studies on the fusion bonding behavior of crystallizable amorphous polymers with fusion bonding temperature between T_g and T_m are rare.

For conventional fusion bonding, a combined squeeze flow and intermolecular diffusion model has recently been proposed by Grewell and Benatar²⁵ to explain the fusion bonding behavior of amorphous polymer with bonding temperatures above T_g and semicrystalline polymer with fusion bonding temperature above T_m . When two polymer interfaces are brought together into intimate contact, healing of the interfaces occurs. When amorphous polymer is heated above T_g or semicrystalline polymer is heated above T_m , polymer chains diffuse across the interface and entangle with other polymer chains. With the increase of the heating time, the degree of healing increases. When healing is completed, polymer chains from each side migrate across the interface. The interface becomes indistinguishable from the bulk material. This is demonstrated in Figure 16.²⁶

For crystallizable amorphous polymer bonded at temperatures between T_g and T_m , the fusion bonding mechanism should be different due to the additional influences from crystallization. Originally, the crystallizable amorphous polymer, prepared by rapid quenching, is nearly completely amorphous. When it

is heated between T_g and T_m , the polymer is softened and the chains at the interface start to interdiffuse with each other. At the same time, with the increase of the heating time, the crystallizable amorphous polymer can crystallize. Crystallization causes the polymer to harden and hinders the interdiffusion.

Using the experimental results from etching, SEM, TEM, polarized microscopy, and peeling test in this study, a fusion bonding model for crystallizable amorphous polymer with bonding temperature between T_g and T_m was proposed, as shown in Figure 17. When two crystallizable amorphous sheets are heated between T_g and T_m and brought into a contact, molecular chains on each side of the interface will diffuse into each other. At the same time, the interface can induce nucleation. Then crystals grow on the interface. These crystals in the vicinity of the interface can induce nucleation in the bulk to form a second interfacial region. Simultaneously, homogeneous crystal nucleation and growth happens in the bulk. Later, with the increase of the heating time, the width of the interfacial region will decrease due to the annealing effects. Therefore, at a higher heating temperature, the width of the interface becomes smaller.

CONCLUSIONS

The fusion bonding morphology of crystallizable amorphous PET sheets was studied using etching techniques, SEM, TEM, and polarized optical microscopy. Double interfacial regions were observed when two crystallizable amorphous PET sheets were bonded together between T_g and T_m . The contact interface of the two PET sheets appeared to serve as a strong nucleating site for the crystallization of PET in the vicinity. Transcrystals were nucleated at the interface. The transcrystals on the interface appeared to induce nucleation in the PET bulk to form the second interfacial region. With the increase of the heating time, the width of the interfacial region decreased. The fusion bonding strength determined by the peeling test was found to be significantly affected by the state of crystallization at the bonding interface. Different from fusion bonding of noncrystallizable amorphous polymer, the peeling strength did not simply increase with the increase of fusion time. Based on the experimental observations, a fusion bonding mechanism of crystallizable amorphous polymer was proposed to explain the interplay between crystallization and interdiffusion in affecting the interfacial morphology and bonding quality.

References

1. Capiati, N. J.; Porter, R. S. *J Mater Sci* 1975, 10, 1671.
2. Matabola, K. P.; Vries, A. R.; Moolman, F. S.; Luyt, A. S. *J Mater Sci* 2009, 44, 6213.

3. Ward, I. M.; Hine, P. J. *Polymer* 2004, 45, 1413.
4. Hine, P. J.; Ward, I. M.; Olley, R. H.; Bassett, D. C. *J Mater Sci* 1993, 28, 316.
5. Kabeel, M. A.; Bassett, D. C.; Olley, R. H.; Hine, P. J.; Ward, I. M. *J Mater Sci* 1994, 29, 4694.
6. Mead, W. T.; Porter, R. S. *J Appl Polym Sci* 1978, 22, 3249.
7. Yao, D.; Li, R.; Nagarajan, P. *Polym Eng Sci* 2006, 46, 1223.
8. Li, R.; Yao, D. *J Appl Polym Sci* 2007, 107, 2909.
9. Cormia, R. L.; Price, F. P.; Turnbull, D. *J Chem Phys* 1962, 37, 1333.
10. Ma, Y.; Zha, L. Y.; Hu, W. B.; Reiter, G.; Han, C. C. *Phys Rev E* 2008, 77, 061801.
11. Lovering, E. G. *J Polym Sci Part A-2 Polym Phys* 1970, 8, 1697.
12. E. I. Du Pont De Nemours and Company (Inventor: Scarlett, A. C). US Patent 2,823,421, 1958.
13. Wunderlich, B. *Macromolecular Physics*; Academic Press: New York, 1973; Vol.2.
14. Folkes, M. J.; Hardwick, S. T. *J Mater Sci Lett* 1987, 6, 656.
15. Hata, T.; Ohsaka, K.; Yamada, T.; Nakamae, K.; Shibata, N.; Matsumoto, T. Proceedings of the 16th Annual Symposium, Adhesion Society, Williamsburg, VA, February 1993; p 180.
16. Kwei, T. K.; Schonhorn, H.; Frisch, H. L. *J Appl Phys* 1967, 38, 2512.
17. Matsuoka, S.; Daane, J. H.; Bair, H. E.; Kwei, T. K. *J Polym Sci B Polym Lett* 1968, 6, 87.
18. Kim, S. G.; Suh, N. P. *Polym Eng Sci* 1986, 26, 1200.
19. Malguarnera, S. C.; Manisali, A. *Polym Eng Sci* 1981, 21, 586.
20. Hagerman, E. M. *Plast Eng* 1973, 29, 67.
21. Hobbs, S. Y. *Polym Eng Sci* 1974, 14, 621.
22. Kausch, H. H. *Polymer Fracture*; Springer: Heidelberg, 1987.
23. Jud, K.; Kausch, H. H. *Polym Bull* 1979, 1, 697.
24. Jud, K.; Kausch, H. H.; Williams, J. G. *J Mater Sci* 1981, 16, 204.
25. Grewell, D.; Benatar, A. *Polym Eng Sci* 2008, 48, 860.
26. Perepezko, J. H.; Hildal, K. *Mater Sci Eng B* 2008, 148, 171.